JACS
JOURNAL OF THE AMERICAN CHEMICAL SOCIETY

Communication

pubs.acs.org/JACS

Stable Cobalt Nanoparticles and Their Monolayer Array as an Efficient Electrocatalyst for Oxygen Evolution Reaction

Liheng Wu,[†,§] Qing Li,[†,§] Cheng Hao Wu,[‡,∥] Huiyuan Zhu,[†,#] Adriana Mendoza-Garcia,[†] Bo Shen,[†] Jinghua Guo,[⊥] and Shouheng Sun*[,†]

[†]Department of Chemistry, Brown University, Providence, Rhode Island 02912, United States

[‡]Department of Chemistry, University of California, Berkeley, California 94720, United States

[∥]Materials Sciences Division and [⊥]The Advanced Light Source, Lawrence Berkeley National Laboratory, Berkeley, California 94720, United States

Supporting Information

ABSTRACT: Monodisperse cobalt (Co) nanoparticles (NPs) were synthesized and stabilized against oxidation via reductive annealing at 600 °C. The stable Co NPs are active for catalyzing the oxygen evolution reaction (OER) in 0.1 M KOH, producing a current density of 10 mA/cm^2 at an overpotential of 0.39 V (1.62 V vs RHE, no *iR*-correction). Their catalysis is superior to the commercial Ir catalyst in both activity and stability. These Co NPs are also assembled into a monolayer array on the working electrode, allowing the detailed study of their intrinsic OER activity. The Co NPs in the monolayer array show 15 times higher turnover frequency (2.13 s^{-1}) and mass activity (1949 A/g) than the NPs deposited on conventional carbon black (0.14 s^{-1} and 126 A/g, respectively) at an overpotential of 0.4 V. These stable Co NPs are a promising new class of noble-metal-free catalyst for water splitting.

Oxygen evolution reaction (OER) is commonly referred to as electrochemical oxidation of "O^{2-}" to O_2. It is an important half-cell reaction and is coupled with hydrogen evolution reaction (HER) in a water-splitting cell for efficient proton reduction and hydrogen (H_2) generation.[1−3] As a thermodynamically "up-hill" reaction that involves multi-electron transfer, it requires the input of energy to drive its completion. In order to lower the reaction energy barrier, an efficient catalyst is needed to promote the four-electron oxidation process and make OER proceed at low overpotentials. For this purpose, nanostructured iridium (Ir) and ruthenium (Ru) have been chosen as the state-of-the-art OER catalysts.[4−10] Recently, earth-abundant transition-metal oxides/hydroxides,[11−21] especially Co-based complexes,[22−25] Co−O-based thin films,[26−29] nanoparticles (NPs),[30−39] and layered structure,[40−45] are also explored as promising alternative catalysts for OER. However, these oxides have generally low electronic conductivity, limiting their potential in electrocatalysis enhancement.

One recent strategy applied to improve the OER catalytic activity of these oxides is to couple them with a conductive support such as graphene,[17] carbon nanotubes,[14,33] metallic Au,[26,46] or even Au NPs, as demonstrated in the core/shell Au/Co_3O_4 structure.[35] These studies indicate that catalytic activity may be further enhanced if the catalyst can be made more electron conductive. Studying the general design of the catalysts, we see that these conductive supports can only offer a partial solution to the desired enhancement in catalysis, as the electron transfer required for the OER on the catalytically active surface may only be possible at the catalyst−support interface, not on the entire catalyst surface. To further enhance the OER activity, the catalyst itself is better conductive to facilitate electron transfer for the OER.[47] This makes metallic Co NPs a promising catalyst choice. However, it is known that metallic Co NPs are chemically unstable, subject to fast oxidation when exposed to air or in an oxygenated solvent. It is therefore essential to stabilize metal Co NPs first before they can be studied for the OER. Herein, we report that when synthesized and treated properly, metallic Co NPs can be stabilized to serve as a new class of efficient catalyst for OER in 0.1 M KOH. Moreover, using a water−air interface self-assembly method, we have assembled these Co NPs into a well-defined monolayer array. The uniform array of Co NPs allows the detailed evaluation of their intrinsic activity for OER. The monolayer catalyst shows about 15 times higher turnover frequency (TOF) and mass activity than the Co NPs deposited on conventional carbon support.

The Co NPs were synthesized through the thermal decomposition of cobalt carbonyl [$Co_2(CO)_8$] in 1,2,3,4-tetrahydronaphthalene solution with oleic acid and dioctylamine as surfactants (see Supporting Information (SI) for experimental details).[48,49] Figure S1 shows a typical transmission electron microscopy (TEM) image of the as-synthesized Co NPs that are monodisperse with the diameter of 10 ± 1 nm. The as-synthesized Co NPs were loaded on Ketjen carbon (C) at an initial mass ratio of 1:1 through sonication of Co NP dispersion and C support in hexane, denoted as C−Co NPs (Figure 1A). Inductively coupled plasma atomic emission spectroscopy analysis confirmed the mass ratio of Co NPs in the C−Co catalyst was 42%. As demonstrated previously,[48] the as-synthesized magnetic Co NPs are not stable and subject to fast oxidation. To improve their stability, these C−Co NPs were annealed in Ar + 5% H_2 at

Received: April 21, 2015
Published: May 27, 2015

DOI: 10.1021/jacs.5b04142
J. Am. Chem. Soc. 2015, 137, 7071−7074

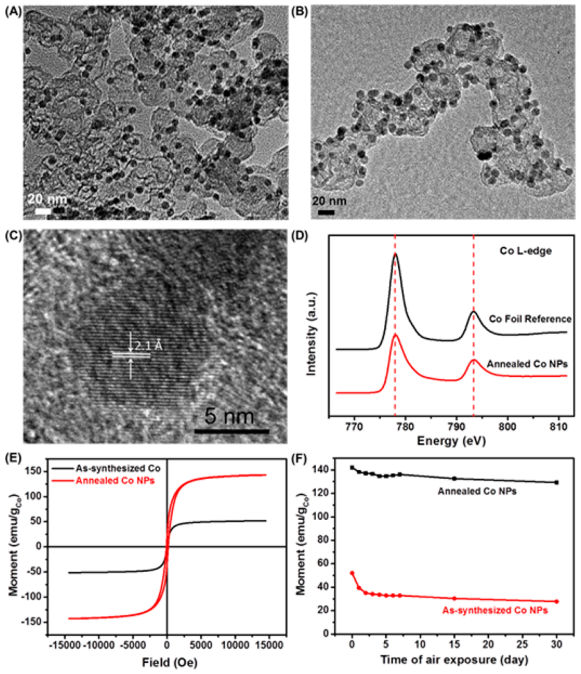

Figure 1. TEM image of (A) the as-synthesized C−Co NPs and (B) the C−Co NPs after reductive annealing in Ar + 5% H_2 at 600 °C for 1 h. (C) HR-TEM image of a representative single Co NP from (B). (D) Ex situ XAS spectra of Co L-edge of the Co reference foil and the annealed C−Co. (E) Room-temperature hysteresis loops of the C−Co NPs before and after reductive annealing. (F) Change of magnetic moment of the Co NPs vs the time of air exposure at room temperature.

600 °C for 1 h. This reductive annealing reduces the surface oxide to metallic Co, increases the Co crystallinity, and removes the surfactants to activate the catalyst for the subsequent electrochemical measurements. The TEM image of the annealed C−Co NPs in Figure 1B indicates no aggregation of the Co NPs on the carbon support. High-resolution TEM (HR-TEM) image of a representative Co NP deposited on C in Figure 1C confirms that the annealed Co NP is indeed well-crystallized with the lattice fringe spacing measured to be 2.1 Å, which is close to the (111) interplanar spacing of the face-centered cubic (fcc) Co. X-ray diffraction pattern (Figure S2) further reveals that the crystallinity of the Co NPs is significantly enhanced after reductive annealing.

Ex situ X-ray absorption spectroscopy (XAS) was applied to study the chemical states of the annealed Co NPs. The XAS measurements were performed in the total electron yield detection mode to make them sensitive to the surface of the Co NPs. The XAS spectrum of the Co L-edge of the annealed Co NPs in Figure 1D shows two peaks at 778.0 and 793.3 eV that match those for the metallic Co reference foil, indicating that the surface of the annealed Co NPs is in metallic nature without obvious surface oxidation. Chemical stability of the metallic C−Co NPs was monitored by the change of their magnetic properties using a vibrating sample magnetometer. Figure 1E is room-temperature magnetic hysteresis loops of the C−Co NPs before and after reductive annealing in Ar + 5% H_2 at 600 °C for 1 h. The magnetic moments were normalized to the mass of Co. Due to the surface oxidation, the initial Co NPs on the carbon support are super paramagnetic with the magnetic saturation moment (M_s) of 52 emu/g. After the reductive annealing, their M_s increases to 142 emu/g, which is close to the bulk Co value (~162 emu/g). The M_s change of the Co NPs exposed to air was monitored, as shown in Figure 1F. The M_s of the as-synthesized Co NPs drops to 39 emu/g after 1 day and further decreases to 28 emu/g after 30 days (46% loss). As a comparison, the annealed Co NPs are much more stable with their M_s staying at 129 emu/g level even after 30 days, indicating that annealing indeed helps to stabilize Co NPs against air oxidation. This stability enhancement is also more significant than that for crystalline bcc-Fe NPs reported previously.[50,51]

The OER activity of the annealed Co NPs was evaluated in O_2-saturated 0.1 M KOH solution using a standard three-electrode system. The C−Co NP catalyst was cast onto the glassy carbon (GC) working electrode. The OER polarization curves were recorded by linear sweep voltammetry at the scan rate of 10 mV/s and continuous rotating speed of 1600 rpm. Figure 2A shows the polarization curves of the annealed C−Co

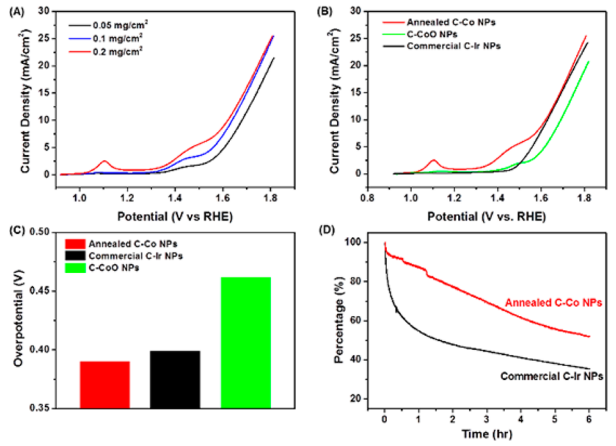

Figure 2. (A) Polarization curves of (A) the annealed C−Co NPs on GC electrode at three different mass loadings and (B) the annealed C−Co NPs, C−CoO NPs and commercial C−Ir catalyst on GC electrode with a mass loading of 0.2 mg/cm^2. Measurements were performed on GC electrode in 0.1 M KOH at the scan rate of 10 mV/s and rotating speed of 1600 rpm. All the polarization curves were collected without *iR*-correction. (C) Comparison of the overpotential for different catalysts at the current density of 10 mA/cm^2. (D) Chronoamperometric curves of the annealed C−Co NPs and commercial C−Ir catalyst on GC electrode at an overpotential of 0.4 V (1.63 V vs RHE) in 0.1 M KOH.

catalyst with three different mass loadings without *iR*-correction. The overpotential at the current density of 10 mA/cm^2, which is normally used for evaluating the electrochemical activity of an OER catalyst,[11,52] decreased from 0.45 to 0.39 V while increasing the catalyst loading from 0.05 mg/cm^2 to 0.2 mg/cm^2. Further increasing the mass loading resulted in thicker catalyst film, causing limited mass transport and detachment of catalyst from the electrode during electrochemical measurement. Thus, the optimal catalyst loading of 0.2 mg/cm^2 was chosen for the further study.

To better evaluate the OER activity of the annealed C−Co NPs catalyst, the commercial Ir catalyst (10 wt % Ir on Vulcan carbon black from Premetek Co., Figure S3) with the same mass loading of 0.2 mg/cm^2 was chosen as a reference. The C-CoO NPs were also studied as a control (see the SI and Figure S4). Their polarization curves are shown in Figure 2B. For the annealed Co NPs, during electrochemical oxidation, the surface metallic Co atoms were oxidized, as indicated by the anodic

DOI: 10.1021/jacs.5b04142
J. Am. Chem. Soc. 2015, 137, 7071−7074

peaks observed at ~1.10 V for oxidation of Co^{II} to Co^{III} and 1.46 V for Co^{III} to Co^{IV}.[26,30] However, the metallic core of the annealed Co NPs increased their electronic conductivity and thus enhanced the catalytic activity. Compared with the insulating CoO NPs, the annealed Co NPs exhibited much higher current density at all potentials and much smaller overpotential at the current density of 10 mA/cm^2 (0.39 vs 0.46 V). The OER activity of the annealed Co NPs is also better than the commercial Ir catalyst. Their overpotentials at the current density of 10 mA/cm^2 are summarized in Figure 2C. It is worth mentioning that all the polarization curves shown here are without any *iR*-correction. If considering the uncompensated resistance of the electrochemical cell, the overpotential of the annealed Co NPs for producing a current density of 10 mA/cm^2 decreased to ~0.3 V after *iR*-correction (Figure S5), which is comparable or even smaller than the values of some other nonprecious catalysts under similar experimental conditions.[14,16,35,42]

The stability of the annealed C−Co NPs and commercial C−Ir NPs was tested by using a chronoamperometric method at an overpotential of 0.4 V (Figure 2D). After 1 h, the current density for the annealed C−Co NPs dropped 13%, while the value from the C−Ir NPs decreased 45%. Even after 6 h test, the C−Co NPs still showed a slower rate of activity decrease than the commercial C−Ir, indicating that the annealed Co NPs are much more stable than the commercial Ir NPs. The NPs in the catalysts were further characterized after the stability test (Figure S6). The Ir NPs are aggregated, while the Co NPs stay well dispersed on the carbon support but have a core/shell structure due to surface oxidation of Co, which explains their slow activity drop over time. We should note that the oxidized Co can be readily reduced back to Co by the same reductive annealing described above and the C−Co catalyst can be regenerated and reused for the OER.

Previous studies have indicated that decreasing the thickness of the catalysts can increase the number of active sites and catalyst's TOF.[18,26] Very recently, self-assembled monolayer or multilayer NP catalysts have been developed for enhanced activity.[53−55] To better evaluate the OER catalysis of the Co NPs, we assembled them into a monolayer array through a water−air interface self-assembly approach.[56−58] The monolayer array could be transferred easily to a carbon-coated TEM grid for TEM analysis (Figure 3A) or to a GC plate (0.6 × 0.7 cm) for scanning electron microscopy (SEM) imaging (Figure S7). The monolayer Co NP array on GC plate was pre-annealed at 600 °C as described and was used as a working electrode; note: no NP aggregation was observed after the annealing treatment. From the TEM/SEM images of the Co NP array (Figures 3A and S7) we estimated the Co NP packing density at ~4000 NPs/μm^2. The Co NP array showed high OER activity (Figure 3B) (the GC plate itself was not active for OER). The TOFs were calculated by assuming that all the surface Co atoms of the 10 nm fcc-Co NPs are catalytically active (see the SI). Figure 3C shows the TOFs at an overpotential of 0.4 V for the Co NP array and the C−Co catalyst with different mass loadings. For the catalyst with a mass loading of 84 μg_{Co}/cm^2 (C−Co NP catalyst at the loading of 0.2 mg/cm^2 with 42 wt % Co), the TOF is 0.14 s^{-1}. However, by decreasing the thickness of the catalyst to the monolayer level (1.1 μg_{Co}/cm^2), the TOF increases by about 15 times to 2.13 s^{-1}. This TOF enhancement is in good agreement with previous reports about the thickness effect on the TOFs.[18,26] Moreover, the mass activity of the monolayer

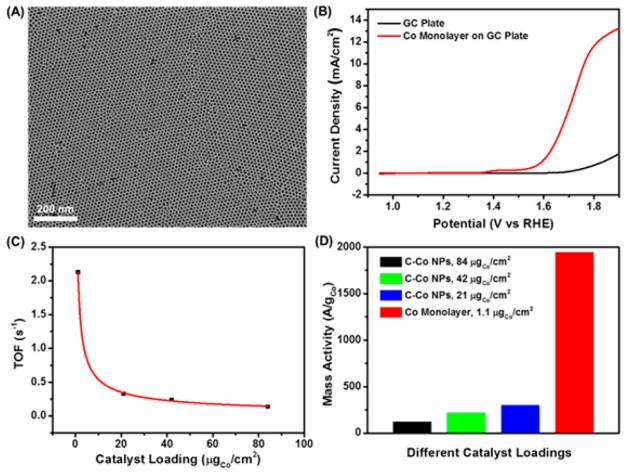

Figure 3. (A) TEM image of the monolayer assembly of Co NPs. (B) Polarization curves of the bare GC plate and the annealed Co NP monolayer catalyst on the GC plate at the scan rate of 10 mV/s in 0.1 M KOH. (C) TOFs and (D) mass activity of the annealed Co NP catalysts with different catalyst loadings at an overpotential of 0.4 V.

catalyst was also evaluated (Figure 3D). Compared to the C−Co NP catalyst at a mass loading of 84 μg_{Co}/cm^2, the monolayer catalyst exhibits a dramatic enhancement in mass activity from 126 to 1949 A/g. This value is also much higher than that of the commercial C−Ir catalyst (500 A/g).

In summary, highly stable metallic Co NPs have been synthesized through a post-reductive annealing process. These metallic Co NPs are more active and durable for OER than the commercial Ir catalyst. The high catalytic efficiency can be ascribed to better electron conductivity of the metallic core. To better evaluate the intrinsic activity of the metallic Co NPs, a monolayer array of Co NPs has been fabricated through Co NP self-assembly at water−air interface. The monolayer NP catalyst exhibits 15 times higher TOF and mass activity than the Co NPs deposited on conventional carbon support. With better activity and stability than the commercial Ir catalyst, these metallic Co NPs should serve as a promising noble-metal-free catalyst for efficient OER in alkaline media.

■ ASSOCIATED CONTENT

Supporting Information

Experimental details, TOF, and mass activity calculations and Figures S1−S7. The Supporting Information is available free of charge on the ACS Publications website at DOI: 10.1021/jacs.5b04142.

■ AUTHOR INFORMATION

Corresponding Author

*ssun@brown.edu

Present Address

[#]Chemical Sciences Division, Oak Ridge National Laboratory, Oak Ridge, TN 37830, United States

Author Contributions

[§]These authors contributed equally.

Notes

The authors declare no competing financial interest.

■ ACKNOWLEDGMENTS

This work was supported by the U.S. Army Research Laboratory and the U.S. Army Research Office under the

DOI: 10.1021/jacs.5b04142
J. Am. Chem. Soc. 2015, 137, 7071−7074

Multi University Research Initiative (MURI, grant no. W911NF-11-1-0353) on "Stress-Controlled Catalysis via Engineered Nanostructures" and by the U.S. Army Research Office (Grant W911NF-15-1-0147) on "New Composite Catalysts Based on Nitrogen-Doped Graphene and Nanoparticles for Advanced Electrocatalysis". C.H.W. acknowledges the ALS Doctoral Fellowship in Residence. The work at the Advanced Light Source was supported by the Office of Basic Energy Sciences of the U.S. Department of Energy under contract no. DE-AC02-05CH11231.

REFERENCES

(1) Subbaraman, R.; Tripkovic, D.; Strmcnik, D.; Chang, K. C.; Uchimura, M.; Paulikas, A. P.; Stamenkovic, V.; Markovic, N. M. *Science* **2011**, *334*, 1256.
(2) Kudo, A.; Miseki, Y. *Chem. Soc. Rev.* **2009**, *38*, 253.
(3) Walter, M. G.; Warren, E. L.; McKone, J. R.; Boettcher, S. W.; Mi, Q. X.; Santori, E. A.; Lewis, N. S. *Chem. Rev.* **2010**, *110*, 6446.
(4) Yagi, M.; Tomita, E.; Kuwabara, T. *J. Electroanal. Chem.* **2005**, *579*, 83.
(5) Fang, Y. H.; Liu, Z. P. *J. Am. Chem. Soc.* **2010**, *132*, 18214.
(6) Lee, Y.; Suntivich, J.; May, K. J.; Perry, E. E.; Shao-Horn, Y. *J. Phys. Chem. Lett.* **2012**, *3*, 399.
(7) Casalongue, H. G. S.; Ng, M. L.; Kaya, S.; Friebel, D.; Ogasawara, H.; Nilsson, A. *Angew. Chem., Int. Ed.* **2014**, *53*, 7169.
(8) Morris, N. D.; Suzuki, M.; Mallouk, T. E. *J. Phys. Chem. A* **2004**, *108*, 9115.
(9) Yagi, M.; Tomita, E.; Sakita, S.; Kuwabara, T.; Nagai, K. *J. Phys. Chem. B* **2005**, *109*, 21489.
(10) Nong, H. N.; Oh, H. S.; Reier, T.; Willinger, E.; Willinger, M. G.; Petkov, V.; Teschner, D.; Strasser, P. *Angew. Chem., Int. Ed.* **2015**, *54*, 2975.
(11) Gorlin, Y.; Jaramillo, T. F. *J. Am. Chem. Soc.* **2010**, *132*, 13612.
(12) Hong, D. C.; Yamada, Y.; Nagatomi, T.; Takai, Y.; Fukuzumi, S. *J. Am. Chem. Soc.* **2012**, *134*, 19572.
(13) Subbaraman, R.; Tripkovic, D.; Chang, K. C.; Strmcnik, D.; Paulikas, A. P.; Hirunsit, P.; Chan, M.; Greeley, J.; Stamenkovic, V.; Markovic, N. M. *Nat. Mater.* **2012**, *11*, 550.
(14) Gong, M.; Li, Y.; Wang, H.; Liang, Y.; Wu, J. Z.; Zhou, J.; Wang, J.; Regier, T.; Wei, F.; Dai, H. *J. Am. Chem. Soc.* **2013**, *135*, 8452.
(15) Gorlin, Y.; Lassalle-Kaiser, B.; Benck, J. D.; Gul, S.; Webb, S. M.; Yachandra, V. K.; Yano, J.; Jaramillo, T. F. *J. Am. Chem. Soc.* **2013**, *135*, 8525.
(16) Gao, M. R.; Sheng, W. C.; Zhuang, Z. B.; Fang, Q. R.; Gu, S.; Jiang, J.; Yan, Y. S. *J. Am. Chem. Soc.* **2014**, *136*, 7077.
(17) Long, X.; Li, J. K.; Xiao, S.; Yan, K. Y.; Wang, Z. L.; Chen, H. N.; Yang, S. H. *Angew. Chem., Int. Ed.* **2014**, *53*, 7584.
(18) Trotochaud, L.; Young, S. L.; Ranney, J. K.; Boettcher, S. W. *J. Am. Chem. Soc.* **2014**, *136*, 6744.
(19) Kenney, M. J.; Gong, M.; Li, Y. G.; Wu, J. Z.; Feng, J.; Lanza, M.; Dai, H. J. *Science* **2013**, *342*, 836.
(20) Kuai, L.; Geng, J.; Chen, C. Y.; Kan, E. J.; Liu, Y. D.; Wang, Q.; Geng, B. Y. *Angew. Chem., Int. Ed.* **2014**, *53*, 7547.
(21) Gao, M. R.; Xu, Y. F.; Jiang, J.; Zheng, Y. R.; Yu, S. H. *J. Am. Chem. Soc.* **2012**, *134*, 2930.
(22) Artero, V.; Chavarot-Kerlidou, M.; Fontecave, M. *Angew. Chem., Int. Ed.* **2011**, *50*, 7238.
(23) Dogutan, D. K.; McGuire, R., Jr.; Nocera, D. G. *J. Am. Chem. Soc.* **2011**, *133*, 9178.
(24) Surendranath, Y.; Lutterman, D. A.; Liu, Y.; Nocera, D. G. *J. Am. Chem. Soc.* **2012**, *134*, 6326.
(25) Kanan, M. W.; Nocera, D. G. *Science* **2008**, *321*, 1072.
(26) Yeo, B. S.; Bell, A. T. *J. Am. Chem. Soc.* **2011**, *133*, 5587.
(27) Trotochaud, L.; Ranney, J. K.; Williams, K. N.; Boettcher, S. W. *J. Am. Chem. Soc.* **2012**, *134*, 17253.
(28) Smith, R. D.; Prevot, M. S.; Fagan, R. D.; Trudel, S.; Berlinguette, C. P. *J. Am. Chem. Soc.* **2013**, *135*, 11580.
(29) Bajdich, M.; Garcia-Mota, M.; Vojvodic, A.; Norskov, J. K.; Bell, A. T. *J. Am. Chem. Soc.* **2013**, *135*, 13521.
(30) Chou, N. H.; Ross, P. N.; Bell, A. T.; Tilley, T. D. *ChemSusChem* **2011**, *4*, 1566.
(31) Masa, J.; Xia, W.; Sinev, I.; Zhao, A. Q.; Sun, Z. Y.; Grutzke, S.; Weide, P.; Muhler, M.; Schuhmann, W. *Angew. Chem., Int. Ed.* **2014**, *53*, 8508.
(32) Zhang, M.; de Respinis, M.; Frei, H. *Nat. Chem.* **2014**, *6*, 362.
(33) Zhao, A. Q.; Masa, J.; Xia, W.; Maljusch, A.; Willinger, M. G.; Clavel, G.; Xie, K. P.; Schlogl, R.; Schuhmann, W.; Muhlert, M. *J. Am. Chem. Soc.* **2014**, *136*, 7551.
(34) Rosen, J.; Hutchings, G. S.; Jiao, F. *J. Am. Chem. Soc.* **2013**, *135*, 4516.
(35) Zhuang, Z. B.; Sheng, W. C.; Yan, Y. S. *Adv. Mater.* **2014**, *26*, 3950.
(36) Ma, T. Y.; Dai, S.; Jaroniec, M.; Qiao, S. Z. *J. Am. Chem. Soc.* **2014**, *136*, 13925.
(37) Liao, L. B.; Zhang, Q. H.; Su, Z. H.; Zhao, Z. Z.; Wang, Y. N.; Li, Y.; Lu, X. X.; Wei, D. G.; Feng, G. Y.; Yu, Q. K.; Cai, X. J.; Zhao, J. M.; Ren, Z. F.; Fang, H.; Robles-Hernandez, F.; Baldelli, S.; Bao, J. M. *Nat. Nanotechnol.* **2014**, *9*, 69.
(38) Jiao, F.; Frei, H. *Angew. Chem., Int. Ed.* **2009**, *48*, 1841.
(39) Esswein, A. J.; McMurdo, M. J.; Ross, P. N.; Bell, A. T.; Tilley, T. D. *J. Phys. Chem. C* **2009**, *113*, 15068.
(40) Zou, X.; Goswami, A.; Asefa, T. *J. Am. Chem. Soc.* **2013**, *135*, 17242.
(41) Zhang, Y.; Cui, B.; Zhao, C. S.; Lin, H.; Li, J. B. *Phys. Chem. Chem. Phys.* **2013**, *15*, 7363.
(42) Song, F.; Hu, X. L. *J. Am. Chem. Soc.* **2014**, *136*, 16481.
(43) Lu, Z. Y.; Wang, H. T.; Kong, D. S.; Yan, K.; Hsu, P. C.; Zheng, G. Y.; Yao, H. B.; Liang, Z.; Sun, X. M.; Cui, Y. *Nat. Commun.* **2014**, *5*, 4345.
(44) Gao, M. R.; Liang, J. X.; Zheng, Y. R.; Xu, Y. F.; Jiang, J.; Gao, Q.; Li, J.; Yu, S. H. *Nat. Commun.* **2015**, *6*, 5982.
(45) Zheng, Y. R.; Gao, M. R.; Gao, Q.; Li, H. H.; Xu, J.; Wu, Z. Y.; Yu, S. H. *Small* **2015**, *11*, 182.
(46) Gorlin, Y.; Chung, C. J.; Benck, J. D.; Nordlund, D.; Seitz, L.; Weng, T. C.; Sokaras, D.; Clemens, B. M.; Jaramillo, T. F. *J. Am. Chem. Soc.* **2014**, *136*, 4920.
(47) Viswanathan, V.; Pickrahn, K. L.; Luntz, A. C.; Bent, S. F.; Norskov, J. K. *Nano Lett.* **2014**, *14*, 5853.
(48) Peng, S.; Xie, J.; Sun, S. H. *J. Solid State Chem.* **2008**, *181*, 1560.
(49) Guo, S.; Zhang, S.; Wu, L.; Sun, S. *Angew. Chem., Int. Ed.* **2012**, *51*, 11770.
(50) Lacroix, L. M.; Huls, N. F.; Ho, D.; Sun, X. L.; Cheng, K.; Sun, S. H. *Nano Lett.* **2011**, *11*, 1641.
(51) Zhang, S.; Jiang, G.; Filsinger, G. T.; Wu, L.; Zhu, H.; Lee, J.; Wu, Z.; Sun, S. *Nanoscale* **2014**, *6*, 4852.
(52) McCrory, C. C.; Jung, S.; Peters, J. C.; Jaramillo, T. F. *J. Am. Chem. Soc.* **2013**, *135*, 16977.
(53) Kang, Y. J.; Ye, X. C.; Chen, J.; Cai, Y.; Diaz, R. E.; Adzic, R. R.; Stach, E. A.; Murray, C. B. *J. Am. Chem. Soc.* **2013**, *135*, 42.
(54) Yamada, Y.; Tsung, C. K.; Huang, W.; Huo, Z. Y.; Habas, S. E.; Soejima, T.; Aliaga, C. E.; Somorjai, G. A.; Yang, P. D. *Nat. Chem.* **2011**, *3*, 372.
(55) Kim, D.; Resasco, J.; Yu, Y.; Asiri, A. M.; Yang, P. D. *Nat. Commun.* **2014**, *5*, 4948.
(56) Dong, A. G.; Chen, J.; Vora, P. M.; Kikkawa, J. M.; Murray, C. B. *Nature* **2010**, *466*, 474.
(57) Wen, T.; Majetich, S. A. *ACS Nano* **2011**, *5*, 8868.
(58) Wu, L.; Jubert, P. O.; Berman, D.; Imaino, W.; Nelson, A.; Zhu, H.; Zhang, S.; Sun, S. *Nano Lett.* **2014**, *14*, 3395.

DOI: 10.1021/jacs.5b04142
J. Am. Chem. Soc. 2015, 137, 7071−7074